Formation of Steady-State Oxygen Gradients In Vitro

Application to Liver Zonation

Jared W. Allen, Sangeeta N. Bhatia

Departments of Bioengineering and Medicine, University of California at San Diego, La Jolla, California; telephone: 858-822-3142; fax: 858-822-4203; e-mail: sbhatia@ucsd.edu

Received 31 July 2002; accepted 26 September 2002

DOI: 10.1002/bit.10569

Abstract: We have developed a perfusion bioreactor system that allows the formation of steady state oxygen gradients in cell culture. In this study, gradients were formed in cultures of rat hepatocytes to study the role of oxygen in modulating cellular functions. A model of oxygen transport in our flat-plate reactor was developed to estimate oxygen distribution at the cell surface. Experimental measurements of outlet oxygen concentration from various flow conditions were used to validate model predictions. We showed that cell viability was maintained over a 24-h period when operating with a physiologic oxygen gradient at the cell surface from 76 to 5 mmHg O_2 at the outlet. Oxygen gradients have been implicated in the maintenance of regional compartmentalized metabolic and detoxification functions in the liver, termed zonation. In this system, physiologic oxygen gradients in reactor cultures contributed to a heterogeneous distribution of phosphoenolpyruvate carboxykinase (predominantly localized upstream) and cytochrome P450 2B (predominantly localized downstream) that correlates with the distribution of these enzymes in vivo. The oxygen gradient chamber provides a means of probing the oxygen effects in vitro over a continuous range of O_2 tensions. In addition, this system serves as an in vitro model of zonation that could be further extended to study the role of gradients in ischemia–reperfusion injury, toxicity, and bioartificial liver design. © 2003 Wiley Periodicals, Inc. *Biotechnol Bioeng* **82:** 253–262, 2003.

Keywords: oxygen gradient; bioreactor; zonation; hepatocyte

INTRODUCTION

Oxygen is an important modulator of cellular function in both normal physiology and disease states. Cells respond to oxygen over a wide range of oxygen environments from anoxia to hyperoxia. Anoxic culture conditions (~0 mmHg O_2) severely limit metabolic pathways, compromise plasma membrane integrity, and eventually lead to cell death by necrosis (Herman et al., 1988). Hypoxic responses (5–15 mmHg O_2) are characterized by shifts to more anaerobic metabolic processes or expression of factors that increase oxygen delivery, such as erythropoietin and vascular endothelial growth factor (Semenza, 1999). Baseline metabolism and function typically occur in normoxic environments (30–90 mmHg O_2), and even in a physiologic regime, oxygen can modulate differentiated cell functions (Jungermann and Kietzmann, 2000). Hyperoxic conditions (>160 mmHg O_2) often result in the formation reactive oxygen species that have been implicated in cell injury via lipid peroxidation and cytokine expression (D'Angio and Finkelstein, 2000). With such diversity in cellular responses to oxygen, the dynamics of tissue oxygenation, including the formation of oxygen gradients that span the ranges described above, need to be evaluated more thoroughly.

Oxygen gradients in physiologic systems play an important role in both maintaining homeostasis and inducing acute cellular response. In the microcirculation, for example, gradients of oxygen and nutrients between capillaries and surrounding tissues provide the key driving forces that allow efficient transport. In addition, angiogenesis in development, tissue repair, tumor growth, and vascular remodeling is potentiated by spatial oxygen gradients and expression of oxygen-responsive genes (Giordano and Johnson, 2001; Harris, 2002). Though many oxygen-dependent responses are associated with extreme oxygen environments (hypoxia or hyperoxia), of interest is the ability of oxygen gradients to modulate cellular functions over a normal physiologic range, as is the case with zonal heterogeneity in the liver.

Liver zonation is characterized by regional variations in cellular function along the length of the sinusoid (the capillary of the liver), from the portal vein to the central vein. Zonal heterogeneity in carbohydrate metabolism allows the liver to function as a "glucostat," maintaining blood glucose levels relatively constant during periods of feeding or fast-

Correspondence to: Sangeeta N. Bhatia, M.D., Ph.D., Microscale Tissue Engineering Laboratory, Department of Bioengineering, EBU1 6605, University of California, San Diego, La Jolla, CA 92093-0412. URL: http://mtel.ucsd.edu

Contract grant sponsors: Whitaker Foundation; Packard Foundation; National Institutes of Health

Contract grant number: NIH DK56966

ing (Jungermann and Thurman, 1992). In addition, the deleterious effects of drugs or toxins, such as carbon tetrachloride, on the liver have zone specificity due to regional differences in gene expression and microenvironment (Lindros, 1997). Gradients of oxygen, hormones, and extracellular matrix are thought to be the primary regulators of these zonal variations in metabolism and detoxification (Fig. 1) (Jungermann and Kietzmann, 2000; Kietzmann and Jungermann, 1997). Historically, zonation has been studied in static culture systems in which hepatocytes are exposed to uniform oxygen and hormone environments classified as either "periportal" or "perivenous". However, tissue oxygenation is a dynamic process that is temporally and spatial dependent. Imposing physiologic gradients in a system that implements convective and diffusion transport comparable to that seen in vivo may help to further elucidate the regulators of liver zonation and the role of oxygen in normal and pathophysiologic processes.

We have developed an in vitro perfusion system that allows exposure of cultured cells to a continuous range of oxygen tensions. Using primary rat hepatocytes, convective and diffusion transport of oxygen was modeled in a small-scale parallel-plate bioreactor and validated by experimental measurement. We demonstrated that controlled oxygen gradients contribute to a heterogenous distribution of protein levels, specifically phosphoenolpyruvate carboxykinase (PEPCK) and cytochrome P450 2B (CYP2B), in bioreactor cultures that correlate with patterns seen in vivo. In addition to the applications to bioreactor design, this system may offer insight into the factors that maintain liver zonation as well as the mechanisms of zonation-dependent metabolism and toxicity.

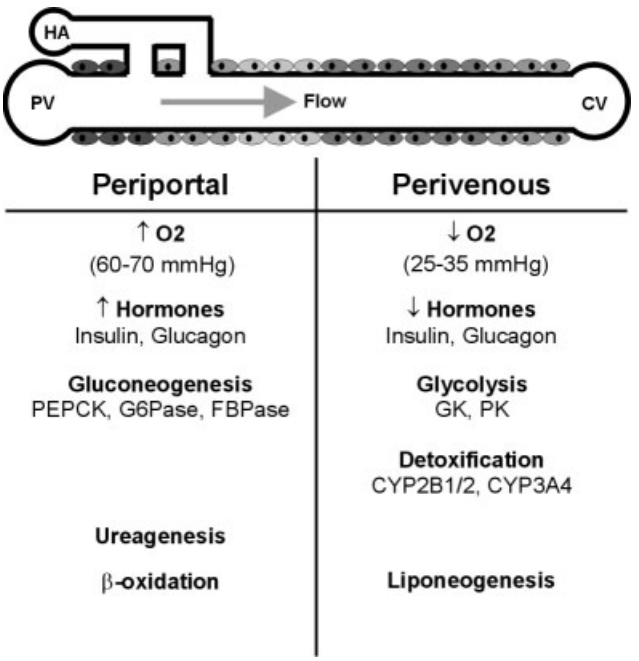

Figure 1. Characteristics of hepatic zonation. The metabolic activity of hepatocytes along the liver sinusoid create oxygen and hormone gradients from the periportal region to the perivenous. As a result, metabolic and detoxification functions are regionally dominant to one zone or the other, as indicated. Some specific markers of each function are listed under each metabolic process. Abbreviations: HA, hepatic artery; PV, portal vein; CV, central vein; PEPCK, phosphoenolpyruvate carboxykinase; G6Pase, glucose-6-phosphatase; FBPase, fructose-1,6-bisphosphatase; GK, glucokinase; PK, pyruvate kinase; CYP, cytochrome P450. Adapted from Kietzmann and Jungermann (1997).

METHODS

Hepatocyte Isolation and Culture

Primary rat hepatocytes were isolated and purified from 2- to 3-month-old adult female Lewis rats (Charles River Laboratories, Wilmington, MA) weighing 180–200 g, by a modified procedure of Seglen (1976). Prior to being seeded, microscope slides (38 mm × 75 mm) were washed in ethanol, rinsed thoroughly with sterile water, and incubated for 1 h at 37°C in a type I collagen solution (0.11 mg/mL). Hepatocytes were cultured on slides to confluency with duplicate seedings of 3×10^6 cells and gentle shaking every 15 min for 1 h after each seeding in media consisting of Dulbecco's Modified Eagle Medium (DMEM, GibcoBRL, Rockville, MD) with 10% fetal bovine serum, supplemented with insulin, hydrocortisone, and antibiotics. Two hours after seeding media was changed to a serum-free formulation of DMEM/Hams' F12 with insulin (5 μg/mL), dexamethasone (10^{-8} *M*), linoleic acid (5 μg/mL), trace elements ($ZnSO_4$, 10^{-10} *M*, $CuSO_4$, 10^{-7} *M*, H_2SeO_3, 3×10^{-10} *M*), and antibiotics. Culture media was buffered with bicarbonate under 5% CO_2 before use in the flow chamber and with 20 m*M* HEPES during chamber experiments. All experiments were performed on day 1 or 2 post-isolation.

Bioreactor and Flow Circuit

A flat-plate bioreactor was designed to conduct experiments using 38 × 75 mm microscope slides. A polycarbonate block was milled to create rectangular inlet and outlet ports in a 100 μm (±10 μm) recess over which a chamber slide could be placed. Slides were sealed in the chamber with inert silicone lubricant (Dow Corning, Midland, MI) and a stainless steel bracket with six screws. The flow field dimensions used in model calculations were 28 mm (width) × 55 mm (length) × 100 μm (height). After assembly, the chamber was inserted to the flow circuit containing a media reservoir, gas exchanger, O_2 probe, and syringe pump (Fig. 2). Pressure-driven flow was continuous using a programmable push-pull syringe pump (Harvard Apparatus, Holliston, MA). Media was equilibrated with 10% or 21% O_2 in a gas exchanger made with gas-permeable silastic tubing. A miniature Clark-type electrode was place at the chamber outlet to measure dissolved O_2 concentration (Microelectrodes, Inc, Bedford, NH). Electrode zeroing was carried out periodically while calibration at the inlet pO_2 was carried out prior to each experiment. Experimental flow rates of recirculating media varied from 0.2 to 4 mL/min. All flow

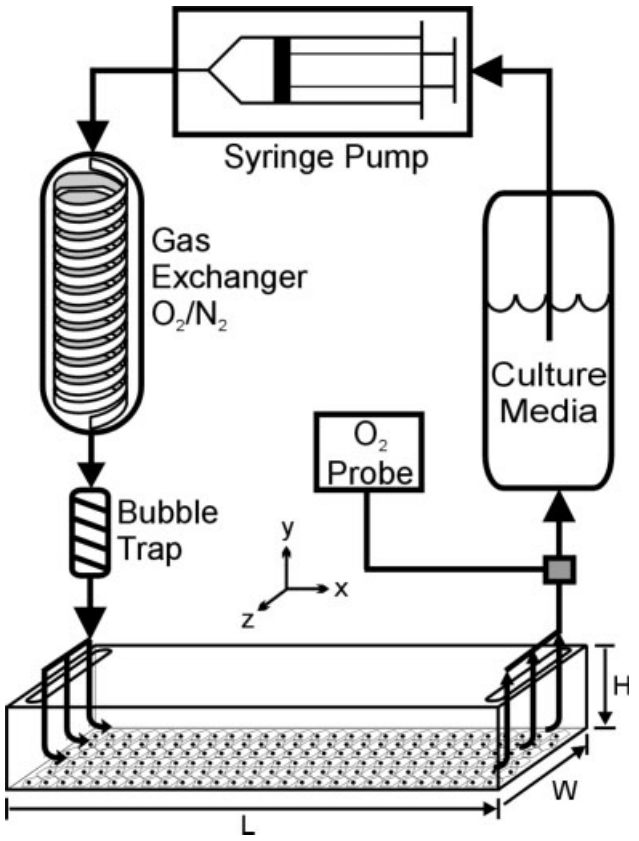

Figure 2. Schematic of experimental apparatus and oxygen transport model geometry of parallel-plate bioreactor.

circuit components except for the syringe pump were housed in a PID-controlled incubator maintained at 37°C.

Microscopy and Immunohistochemistry

Images were obtained using a Nikon Eclipse TE200 inverted microscope, SPOT digital camera (Diagnostic Instruments, Sterling Heights, MI), and Metamorph Image Analysis System (Universal Imaging, Downingtown, PA). Viability was assessed by fluorescence after 24 h of perfusion using Hoechst dye 33258 (nuclear: ex365/em458), fluorescein diacetate (viable: ex494/em516), and propidium iodide (non-viable: ex536/em617). Percent viability was determined by calculating total non-viable cell number and total cell number averaged from 3 fields of the chamber inlet, midline, and outlet.

Regional hypoxia in hepatocyte cultures was shown using the Hypoxyprobe Kit (NPI, Inc, Belmont, MA). This kit uses a probe, pimonidazole hydrochloride, which forms adducts with cellular proteins when pO_2 is below 10 mmHg. Cultures were perfused with media supplemented with Hypoxyprobe-1 (0.11 m*M*) for 3 h and then fixed with 4% paraformaldehyde in PBS. Samples were incubated with monoclonal antibody specific to Hypoxyprobe-1. Secondary staining methods were carried out using a DAKO labeled Streptavidin-Biotin staining kit (DAKO Corporation, Carpinteria, CA).

Zonal Induction

Historically, recapitulation of periportal-like and perivenous-like cell populations in vitro requires simultaneous stimulus by soluble factors and oxygen. Bioreactor cultures were perfused with media and allowed to reach steady state before the addition of inductive agents of glucagon for PEPCK up-regulation or phenobarbitol (PB) and EGF for CYP2B1 induction. Media supplemented with 10 n*M* glucagon was perfused for 8 h allowing for the cAMP-dependent induction of PEPCK before cell lysis (Hellkamp et al., 1991). Media with 0.75 m*M* PB and 0.16 n*M* EGF was perfused for 36 h to induced CYB2B expression before cell lysis (Kietzmann et al., 1999). Cell lysates were collected at the end of each experiment for electrophoretic analysis.

Western Blot Analysis

Primary rat hepatocytes from 6-well plates or chamber slides were lysed and scraped in SDS buffer [10 m*M* Tris/HCl (pH 7.4), 0.1% SDS]. Samples were added to microcentrifuge tubes with 5 μL of PMSF, homogenized with a pestle, and centrifuged at 16,200*g* for 5 min. Total protein content in the supernatant was determined using the DC protein assay (Bio-Rad, Hercules, CA) and used to normalized sample loading. Samples prepared in sample buffer were loaded (10–20 μg/well) for electrophoresis on a 10% polyacrylamide gel. After overnight transfer on to a PVDF membrane, blots were incubated with a blocking buffer [20 m*M* Tris/HCl (pH 7.4), 500 m*M* NaCl, 0.1% Tween 20, and 5% (w/v) milk powder] and washed with buffer without milk powder. Incubation for 1 h with primary antibody against rat PEPCK (gift of Dr. Daryl Granner, Vanderbilt University) or rat CYP2B (Gentest, Woburn, MA) was followed by washing and incubation with either anti-sheep (PEPCK) or anti-goat (CYP2B) HRP-conjugated secondary antibody for 45 min. After washing, the Pierce SuperSignal chemiluminescence reagent was used for detection. All electrophoresis gels were run with molecular mass markers to verify PEPCK bands (67 kDa) or CYP2B1/2 bands (56 kDa). Optical density measurements were obtained using scanned blot images with 1-D gelscan software (Metamorph).

Statistics and Data Analysis

Statistical analysis and model computations were performed using Mathcad (Mathsoft, Inc. Cambridge, MA), which provides a symbolic interface for evaluating the analytical solution (Eq. (7)). Matlab (Mathworks, Inc., Natick, MA) was used to formulate and analyze the numerical solution. Model and experimental data were plotted using Sigmaplot (SPSS, Inc., San Rafaael, CA). Error was reported at the standard deviation of the mean and statistical significance was determined using one-way ANOVA ($P < 0.05$).

Bioreactor Model

The transport of oxygen in a parallel-plate bioreactor can be modeled using the equation of continuity for a binary system. By assuming steady-state transport in a uniform flow field in the x direction and lateral diffusion in the y direction, the non-dimensional governing equation is obtained (Eq. (1)):

$$\frac{\partial \hat{c}}{\partial \hat{x}} = \frac{\alpha}{Pe}\frac{\partial^2 \hat{c}}{\partial \hat{y}^2}, \qquad 0 \le \hat{x} \le 1, \qquad 0 \le \hat{y} \le 1, \qquad (1)$$

where $\hat{c}$ is the dimensionless concentration with respect inlet O_2 concentration, c_{in} ($\hat{c} = [c - c_{in}]/c_{in}$), and $\hat{x}$ and $\hat{y}$ and are non-dimensionalized using the chamber height (H) and chamber length (L) according to $\hat{x} = x/L$ and $\hat{y} = y/H$. The Peclet number, a ratio of convective and diffusive transport, is defined as $\mathrm{Pe} = u_m H/D$, where u_m is the mean velocity, D is oxygen diffusivity, and $\alpha = L/H$. The boundary conditions are given in Eqs. (2–4):

$$\frac{\partial \hat{c}}{\partial \hat{y}}(\hat{x}, 0) = 0, \qquad 0 \le \hat{x} \le 1, \qquad (2)$$

$$\frac{\partial \hat{c}}{\partial \hat{y}}(\hat{x}, 1) = -Da, \qquad 0 \le \hat{x} \le 1, \qquad (3)$$

$$\hat{c}(0, \hat{y}) = 1, \qquad 0 \le \hat{y} \le 1. \qquad (4)$$

Inherently, boundary conditions assume no oxygen flux at the top of the chamber, constant flux at the cell surface, and a constant inlet oxygen concentration. The Damkohler number (Da), the dimesionless oxygen flux, is the ratio of the oxygen uptake rate and diffusion rate as shown in Eq. (5):

$$Da = \frac{\rho V_{max} H}{D c_{in}}, \qquad (5)$$

where ρ is the cell density and V_{max} is the maximal oxygen uptake rate. The model parameters used in calculation are listed in Table I.

Eqs. (1–4) constitute a linear, homogeneous differential equation with a non-homogeneous boundary condition that may be solved analytically. It is assumed that the solution is a combination of the convection-free solution and a homogeneous convection–diffusion solution as given by:

$$\hat{c}(\hat{x}, \hat{y}) = \hat{u}(\hat{x}, \hat{y}) + \hat{v}(\hat{x}, \hat{y}). \qquad (6)$$

Table I. Modeling parameters (Foy et al., 1994).

Parameter	Value	Units
D, O_2 diffusivity	2×10^{-5}	cm^2/s
V_{max}, max. O_2 uptake	0.38	$nmol/s/10^6$ cells
K_m, Michaelis constant	5.6	mmHg
ρ, cell density	1.7×10^5	$cells/cm^2$
c_{in}, inlet O_2 conc.	90–190	nmol/mL
Q, volumetric flowrate	0.3–3	mL/min
H, height	100	μm
W, width	2.8	cm
L, length	5.5	cm

The convection-free solution, $\hat{u}(\hat{x}, \hat{y})$, is a polynomial expression that satisfies Eq. (1) and the boundary conditions. The second term, $\hat{v}(\hat{x}, \hat{y})$, is derived by applying Fourier's method. The complete solution for the oxygen concentration profile is shown in Eq. (7).

$$\hat{c}(\hat{x}, \hat{y}) = Da\left[\frac{1 - 3\hat{y}^2}{6} - \frac{\alpha}{\mathrm{Pe}}\hat{x} + \frac{2}{\pi^2}\sum_{n=1}^{\infty}\frac{(-1)^2}{n^2}\exp\left(-\frac{\alpha n^2 \pi^2 \hat{x}}{\mathrm{Pe}}\right)\cos(n\pi\hat{y})\right]. \qquad (7)$$

The boundary condition given in Eq. (3) assumes constant oxygen uptake along the entire length of the chamber. Michaelis–Menten kinetics more accurately predict oxygen uptake in rat hepatocytes, especially at low oxygen concentrations. Thus, a numerical solution for Eq. (1) was obtained using a Crank–Nicholson finite differencing scheme, with first-order discretization at the boundaries and an explicit approximation of the Michaelis–Menten equation (Press, 1992). Numerical results were compared to the closed form solution (Eq. (7)) to ensure consistency.

RESULTS

Model Output

The objective of the perfusion experiments was to impose a controlled oxygen gradient over the cultured hepatocytes in order to modulate their function. Eq. (7) was used to predict the oxygen concentration profile along the length of the chamber. Figure 3 demonstrates a contour plot of the O_2 distribution in the cross-section of the bioreactor (inlet pO_2 = 158 mmHg, Q = 0.35 mL/min). The oxygen profile can be seen as a combination of oxygen diffusion to the cell surface with constant uptake and convection in the x direction. As the Peclet number is dependent on flow rate (proportional to mean longitudinal velocity, v_m), it follows from the governing equation (Eq. (1)) that convective transport would dominate with increasing flow rate while diffusion transport becomes more important as flow approaches zero.

As a result, it is expected that lower flow rates allow sufficient diffusion to surface to induce oxygen gradients along the length of the bioreactor. Figure 4A shows the flow rate dependence of oxygen concentration at the cell surface. Two regions are depicted that correspond to typical physi-

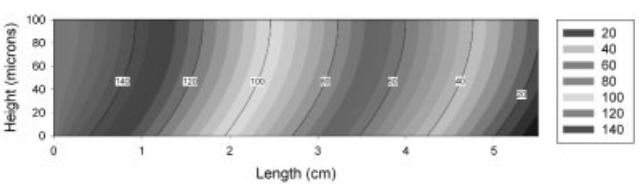

Figure 3. Two-dimensional contour plot of predicted oxygen concentration profile in bioreactor cross-section. Output shows oxygen distribution with inlet pO_2 of 158 mmHg and flow rate 0.35 mL/min (Re = 0.3) using the experimental parameters listed in Table I.

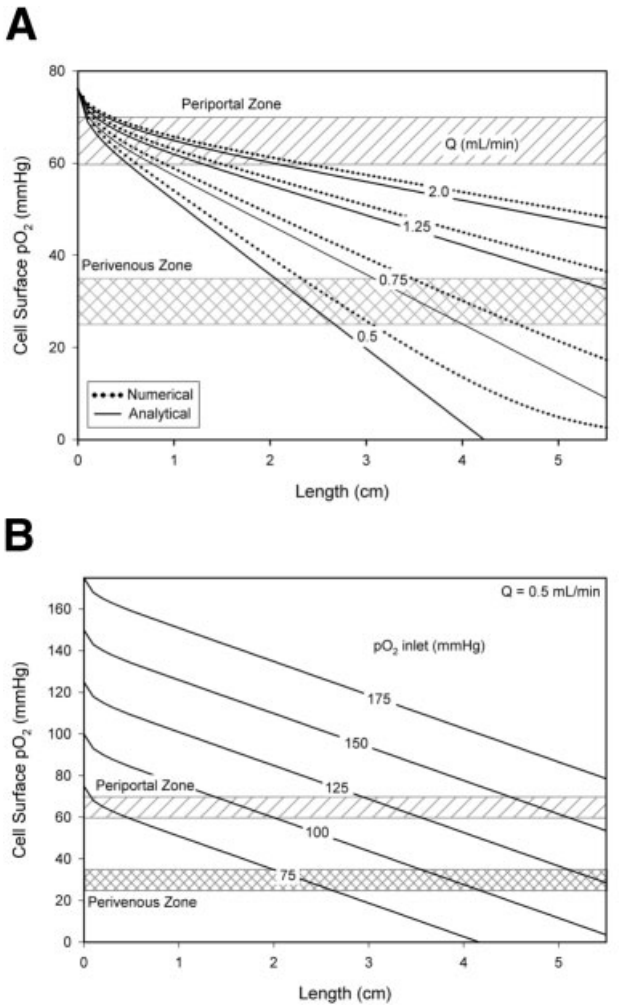

Figure 4. Comparison of oxygen transport model. (**A**) Flow rate dependence of bioreactor oxygen gradients. Model output for flow rate ranging from 0.5 to 2 mL/min with a fixed inlet pO_2 of 76 mmHg is shown for both the analytical and numerical solutions to Eq. (1). (**B**) Inlet pO_2 dependence of bioreactor oxygen gradients. With a fixed flow rate of 0.5 mL/min, the effect of various inlet pO_2 from 75 to 175 mmHg is shown from the analytical solution. Regions of oxygen tension that correspond to typical periportal and perivenous O_2 levels are depicted.

ologic oxygen partial pressures found in the periportal zone (60–70 mmHg) and perivenous zone (25–35 mmHg) of the liver. Under optimal operating conditions, the transition from a periportal to a perivenous oxygen environment would occur at the midline (2.25 cm) and cell surface oxygen concentration would not drop below a critical value of 5 mmHg. Given an inlet oxygen concentration of 76 mmHg (10% O_2), the optimal range of volumetric flow rate is 0.5 to 0.75 mL/min where the final 50% of chamber length could be exposed to perivenous oxygen levels (<35 mmHg). Similar analysis for an oxygen inlet pO_2 of 158 mmHg (21% O_2) indicates that operating at 0.3 mL/min subjects 25% of the chamber near the outlet to perivenous levels without hypoxia.

Figure 4A also emphasizes the differences between the analytical and numerical solutions of Eq. (1). Deviations occur most significantly in regions of low pO_2 due to the assumption in the analytical solution that oxygen consumption is independent of concentration (Eq. (4)). With the application of Michaelis–Menten oxygen uptake kinetics at the boundary, the numerical solution accounts for concentration-dependent changes in oxygen demand. When the bioreactor is operated without oxygen limitations, such as is the case at 2.0 mL/min and above, the constant oxygen uptake assumption holds and better correlation is seen between analytical and numerical solutions.

Inlet oxygen concentration is another system parameter that may be used to modify bioreactor conditions. Figure 4B shows the dependence of cell-surface oxygen concentration on inlet concentration at a fixed flow rate of 0.5 mL/min. As shown, the slope of the oxygen gradient is not affected, but changing inlet concentration shifts the absolute magnitude linearly. Though increasing the inlet oxygen concentration offers a wider range of operating conditions, physiological levels of oxygen below 90 mmHg are effectively applied across the entire culture with lower inlet concentrations. Experiments presented herein were performed with inlet partial pressures ranging from 76 to 158 mmHg.

Validation of Bioreactor Oxygen Gradients

To verify the presence of oxygen gradients in the hepatocyte bioreactor, outlet oxygen levels were monitored and compared to predicted values. Outlet oxygen tension was measured as a function of flow rate, ranging from 0.4 to 3 mL/min. In single experiments, flow rates were changed every 15–30 min and allowed to reach steady state, at which point O_2 levels were recorded. By way of observation, output pO_2 levels became steady 2–3 min after a change in flow rate. In addition, experiments were conducted over a 4-h period, at the conclusion of which electrode drift was assessed and found to be less than 5% (data not shown). Measured values were plotted against model predictions for two separate inlet oxygen conditions: 76 and 158 mmHg (Fig. 5). Results are the average and standard deviation of three separate validation experiments. Measured oxygen concentration correlated well with the analytical and numerical models. At lower flow rates and lower oxygen partial pressures, the numerical solution was a better estimation of outlet pO_2, as expected. Increased error in measurements was also noted at lower flow rates and may be due to electrode limitations.

Bioreactor cultures were subjected to a gradient that predicted a hypoxic environment ($pO_2 < 10$ mmHg) to 50% of the bioreactor culture. Procedures were followed for application of the Hypoxyprobe kit (see Methods) with an inlet pO_2 of 76 mmHg and flow rate of 0.3 mL/min. In general, staining intensity indicating hypoxia gradually increased along the length of the chamber. Bright-field images in Fig. 6 showed a significant increase hypoxia in the outlet region (B) over the inlet (A).

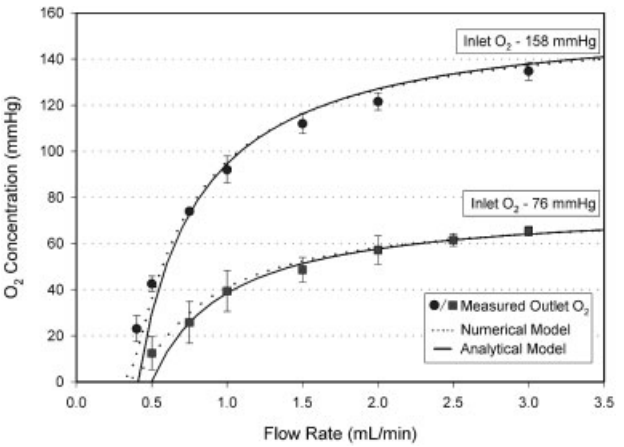

Figure 5. Experimental validation of oxygen transport model. Measured outlet oxygen concentration was measured as a function of flow rate at inlet pO_2 of 76 and 158 mmHg and compared to predicted values. Both the analytical and numerical model predictions are represented. Data points represent the mean and SEM of three separate experiments.

Bioreactor Morphology and Viability

To evaluate possible hepatocyte necrosis due to decreased oxygen availability, bioreactor cultures were perfused for 24 h at 0.35 mL/min with 158 mmHg inlet pO_2. The predicted outlet pO_2 under these conditions is 8 mmHg, and measured levels were 15 ± 3 mmHg after 4 h. After 24 h, images were acquired to assess morphology and viability using methods previously described. Phase images at the inlet, midline, and outlet showed that normal polygonal morphology and bile canaliculi were maintained (Fig. 7A, C, E). Fields from each of the three regions were taken to quantitate viability. The average and standard deviation from three fields are shown in Fig. 7B, D, and F. Results indicated that over a 24-h period viability at the outlet was 85% but statistically was not significantly different from the inlet and middle regions. It was anticipated that these moderate changes in viability would not have an effect on cellular response to zonal induction of PEPCK and CYP2B.

Induction of Zonal Characteristics in Bioreactor Cultures

In vivo, PEPCK is predominately found in periportal regions that contain higher O_2 levels. In the bioreactor system, higher PEPCK levels would be expected in the inlet region when operating with a media flow rate of 0.5 mL/min, which results in a cell surface oxygen gradient of 76 to 5 mmHg from inlet to outlet (Fig. 8A). Western blot analysis of 4 separate bioreactor regions showed maximal PEPCK protein levels at the inlet decreasing to half maximal at the outlet (Fig. 8B). The depletion of O_2 in the bioreactor was responsible for the oxygen gradient, but the depletion of glucagon, which up-regulates PEPCK expression, may also have contributed to the regional variations in PEPCK. To evaluate the possibility of a glucagon gradient contributing to a PEPCK gradient, the bioreactor was operated with inlet

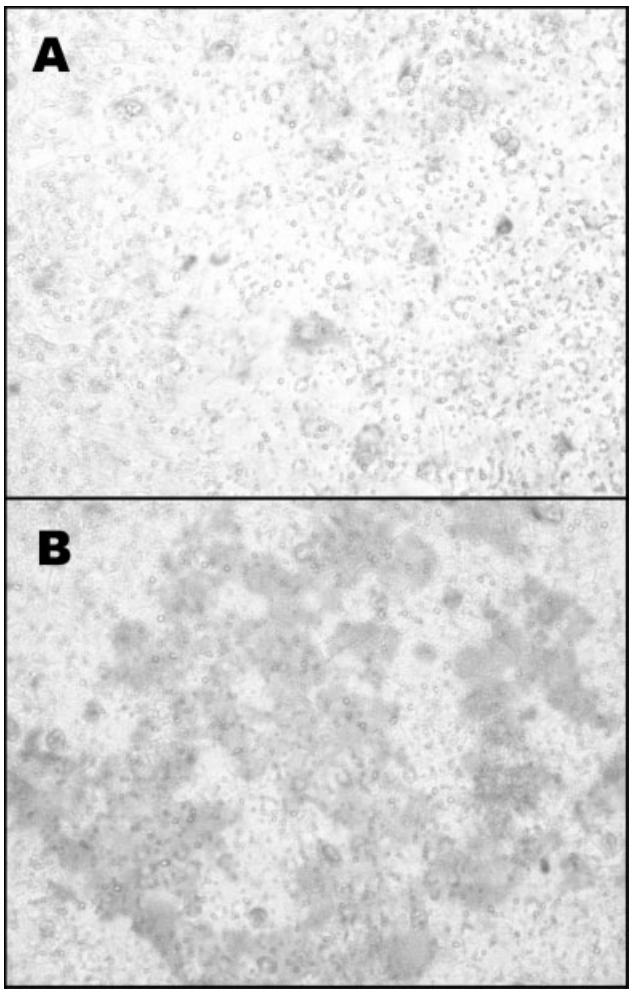

Figure 6. Validation of hypoxic cellular environment at bioreactor outlet. Bioreactor was operated at 0.3 mL/min with inlet pO_2 of 76 mmHg. Higher intensity stain in outlet region (**B**) over the inlet (**A**) indicates the presence of a local hypoxic environment.

pO_2 of 158 mmHg and the same flow rate, 0.5 mL/min. Under this supraphysiologic gradient, the heterogenous induction of PEPCK was abrogated, indicating that oxygen was likely to be the primary modulator of differential PEPCK protein levels in this system. In addition, experiments conducted with higher flow rates resulting in nominal oxygen gradients also showed relatively uniform PEPCK induction (data not shown).

Similarly, low oxygen environments are thought to contribute to the pericentral localization of CYP2B in vivo. The heterogeneous induction of CYP2B in the bioreactor was carried out under a physiologic oxygen gradient with 76 mmHg inlet pO_2 and 0.5 mL/min (Fig. 8A). CYP2B levels were minimal at the chamber inlet and steadily increase to maximal induction in the low O_2 outlet region (Fig. 8C). EGF has been shown to be an inhibitor of CYP2B induction, and as is the case with glucagon, EGF depletion may result in a decreasing EGF gradient. Hence, the observed results may result, in part, from minimized inhibitory effects of CYP2B expression in the outlet region. To test this possi-

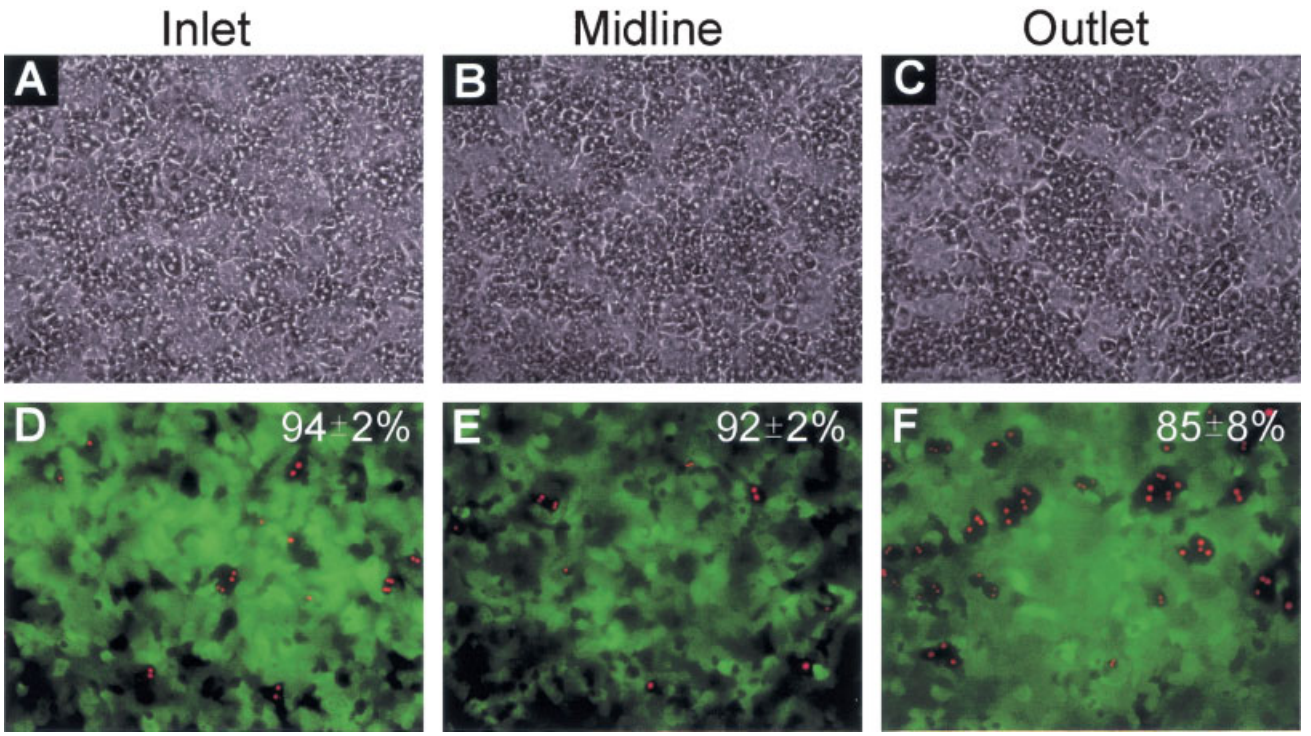

Figure 7. Analysis of morphology and viability in bioreactor cultures. Representative phase-contrast micrographs (**A**, **C**, **E**) from three regions of the bioreactor used for morphology analysis. Fluorescence images (**B**, **D**, **F**) indicating culture viability, reported as the mean ± SEM from three distinct image fields. Images were acquired after 24-h perfusion at 0.35 mL/min with 158 mmHg inlet pO_2. Changes in viability along the length of the chamber were not statistically significant ($P < 0.05$).

bility, supraphysiologic gradients were imposed under the same flow rate that produced graded CYP2B levels and where EGF gradients were presumably similar. Under these conditions and in additional experiments at high flow rate without significant oxygen gradients (data not shown), uniform CYP2B levels were observed. Therefore, physiologic O_2 gradients were explicitly demonstrated to play a role in the induction of zonal CYP2B distributions.

DISCUSSION

In the present study, we developed a bioreactor system that enables the formation of steady state oxygen gradients due to cellular uptake. Specifically, oxygen gradients were applied to cultures of rat hepatocytes to develop and in vitro model of liver zonation. We developed and validated model of oxygen transport considering both analytical and numerical solutions to the governing equation (Eq. (1)) derived from species continuity assumptions. Cells experienced oxygen conditions ranging from normoxia to hypoxia without compromising viability as shown by morphology and fluorescent markers of membrane integrity (Fig. 7). We demonstrated that hepatocytes exposed to oxygen gradients exhibited characteristics of in vivo zonation upon induction as shown by PEPCK (predominantly upstream) and CYP2B (predominantly downstream) protein levels. With this in vitro model of liver zonation, the microenvironmental conditions seen in the liver sinusoid that are thought to be responsible for heterogeneous distribution of metabolic and detoxifying functions can be reproduced.

Bioreactor Design

Perfusion bioreactor systems, particularly those containing hepatocytes, are typically evaluated with respect to design criteria such as reactor geometry, flow parameters, and nutrient transport. Our parallel-plate bioreactor offers a simple Cartesian geometry that provides a uniform flow field in which transport phenomena can be easily modeled. Small-scale, experimental reactors such as this one have an additional advantage of allowing in situ analysis of cellular responses at the molecular level as well as bulk functional assays. However, this system is limited to short term experimentation (3–4 days) due to the use of monolayer cultures of primary hepatocytes, which quickly lose their differentiated function. This shortcoming could be averted with the application of more stable culture models such as collagen gel overlay or co-cultivation with non-parenchymal cells (Bader et al., 1995; Bhatia et al., 1999; Powers et al., 2002; Tilles et al., 2001). When considering flow characteristics, there is often a trade off between providing adequate perfusion and avoiding deleterious fluid shear effects. In addition, both oxygen distribution and fluid shear stress are a highly dependent on the height of the chamber.

Variations in cell seeding conditions and cell height may cause non-uniformity in the flow field and deviations from model predictions. Studies using a similar bioreactor system with various chamber heights reported that albumin synthesis and urea production of rat hepatocytes decreased when exposed to wall shear stresses greater than 5 dynes/cm^2 (Tilles et al., 2001). In our bioreactor, experiments were typically conducted at a flow rate of 0.5 mL/min, corresponding to a shear stress of 1.25 dyne/cm^2, although higher stress near 7.5 dynes/cm^2 may have been present at higher flow rates during validation experiments. Finally, hepatocyte bioreactors, principally those being developed to provide bioartifical liver (BAL) support, require adequate oxygen transport to sustain metabolic function (Hay et al., 2001). Current oxygenation strategies in BAL systems typically preoxygenate inlet streams to supraphysiologic levels (~228 mmHg) to avoid transport limitation, not taking into account to ability of oxygen to modulate function (Custer and Mullon, 1998). Ironically, the high oxygen uptake rate that leads to transport limitations in these larger-scale systems is the same principle by which steady-state gradients are created in our bioreactor, allowing modulation of cell function. While other modeling studies have demonstrated that extreme oxygen limitations would lead to the functional demise of hepatocyte reactors (Ledezma et al., 1999), experiments in our system revealed that viability and responsiveness to hormonal signaling could be sustained even at pO_2 near 5 mmHg. Based on the variations in metabolic and detoxification enzymes induce by oxygen gradients in our system, consideration of the role of oxygen gradients in current BAL or other bioreactor systems may be warranted.

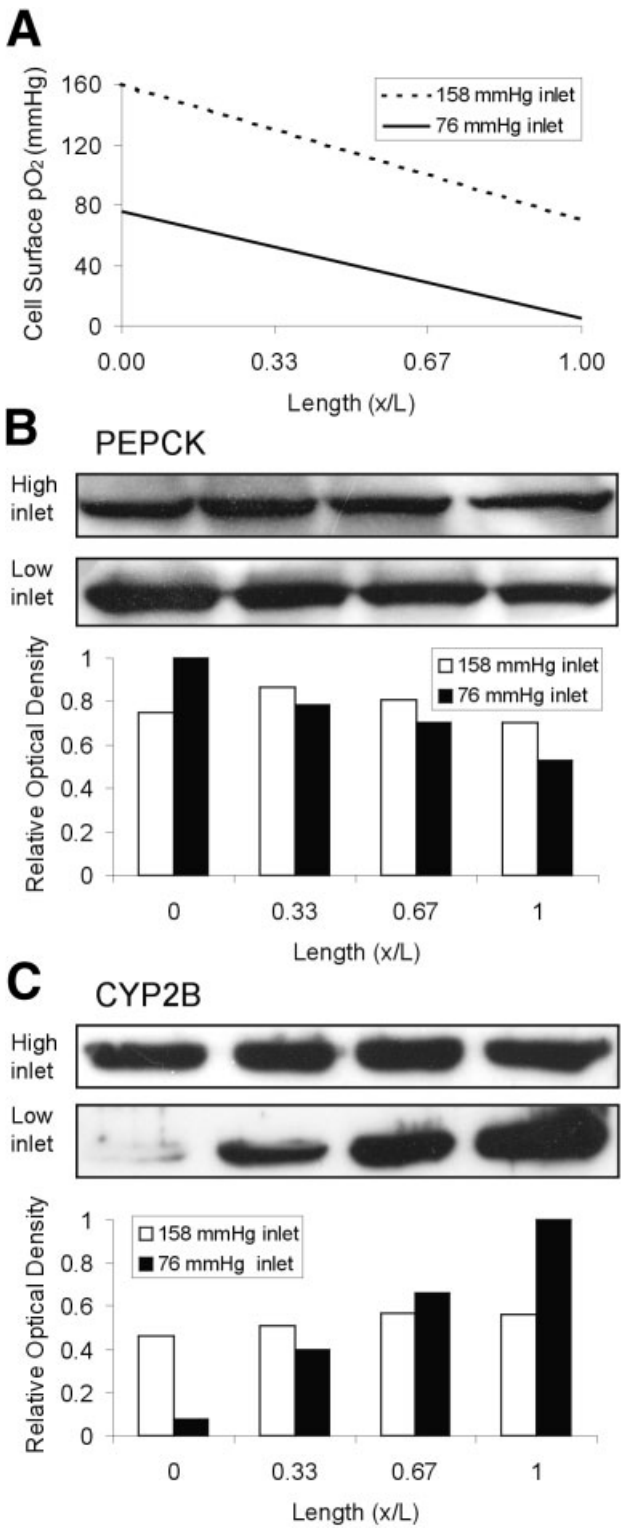

Bioreactor Modeling and Performance

Oxygen measurements were taken over a wide range of flow conditions with two different inlet pO_2 levels (Fig. 5) to show that oxygen gradients could be predicted and controlled to achieve a desired profile. Both analytical and numerical solutions were evaluated for purposes of comparing assumptions about oxygen uptake rate in hepatocytes. The analytical solution (Eq. (7)) to the model overestimated oxygen consumption in low oxygen environments due to the assumption of constant oxygen uptake. A numerical solution that incorporated an explicit approximation of Michaelis–Menten oxygen consumption kinetics more closely correlated with measured values. Though oxygen uptake in rat hepatocytes has been reported to decline after isolation in monolayer culture, our model did not take into account these changes and thus assumed constant V_{max} and K_m values (Table I) that have been reported for day 1 post-isolation

Figure 8. Heterogenous induction of PEPCK and CYP2B by oxygen gradients. Bioreactors were operated with an inlet pO_2 of 76 and 158 mmHg and flow rate of 0.5 mL/min. The resulting in the cell surface oxygen gradients are shown schematically as calculated from the numerical model (**A**). Western blots of PEPCK (**B**) and CYP2B (**C**) protein levels from four regions along the chamber were analyzed to determine relative optical density. In both cases, when the bioreactor was operated with physiologic gradient (low inlet), a heterogeneous induction was observed, whereas imposing a supraphysiologic gradient (control, high inlet) resulted in a more uniform protein distribution. Blots were processed in separate experiments, enabling only qualitative comparison between conditions. Normalization of band densities to the maximal density from both experiments is meant to facilitate comparison.

(Foy et al., 1994). In addition, the challenge of obtaining nearly confluent monolayers of hepatocytes on chamber slides resulted in variability in the cell density parameter, which was estimated from initial cell seeding concentrations and projected surface area calculations. Our experience showed that physiological oxygen gradients (76 mmHg pO_2 inlet) provided more favorable and reproducible operation due the sensitivity of the gradient slope to small changes in flow rate with higher inlet conditions (158 mmHg pO_2 inlet). The advantage of implementing physiological gradients was seen in operational optimization as well as in the induction of zonal functions modulated by oxygen. Future, more precise validation of this system might utilize microelectrode arrays or thin-layer ruthenium sol-gel coatings to study in situ oxygen gradients in detail (Murtagh et al., 1998; Sargent and Gough, 1991).

In Vitro Zonation

It has been shown previously in vitro that oxygen can modulate glucagon-dependent activation of the PEPCK gene (Hellkamp et al., 1991). Though PEPCK activation occurs mainly via a cAMP secondary signal to glucagon binding, the mechanisms by which oxygen can modulate activation is still being elucidated (Bratke et al., 1999). In our in vitro system, we demonstrated that when exposed to a continuous range of oxygen concentrations, rat hepatocytes could exhibit a heterogeneous distribution of PEPCK that correlates with periportal and perivenous localization seen in vivo (Giffin et al., 1993). Control experiments showed that in the absence of a physiologic oxygen gradient, glucagon-dependent PEPCK activation was uniform along the length of the reactor chamber. In addition, though not explicitly measured, glucagon gradients may have been present, but did not appear primarily responsible for the observed heterogenous PEPCK distribution. Further investigation and modeling of hormone gradients in tandem with oxygen gradients may provide insight into the factors contributing to the in vivo zonal distribution of PEPCK, or zonated metabolic enzymes such as pyruvate kinase, glucose-6-phosphatase, or glucokinase.

Several cytochrome P450 isoenzymes have been localized to perivenous regions of the liver (Baron et al., 1981; Lindros, 1997). The induction of CYP2B by phenobarbital has also been shown to be modulated by EGF and oxygen. Studies by Kietzmann et al. (1999) indicated that EGF repression of the PB-dependent induction of CYP2B is lost under perivenous pO_2, resulting in zonal expression pattern that correlates with the in vivo distribution. Consistent with this finding, our in vitro system showed increasing CYP2B induction along the length of the chamber when exposed to PB and EGF, with maximal induction in the low-oxygen perivenous-like region. Under the given operating conditions, an EGF gradient may be contributing to the zonal pattern of CYP2B, in as much as repression of PB-dependent CYP2B activation would be strong in the inlet region and weak at the EGF-depleted outlet region. However, imposing a supraphysiologic oxygen gradient with the same EGF profile did not result in significant differences in CYP2B levels from inlet to outlet, indicated that oxygen was primarily responsible for heterogeneous CYP2B distribution. Further studies examining zonal detoxification could use this same methodology to induce heterogeneous distributions of other P450 isoenzymes such as CYP3A4 or CYP2E1. In addition, with tight control of flow parameters, the kinetics of zonal induction, both for metabolic and detoxification processes, could be examined by retrograde perfusion methods that have been established in whole liver perfusion models (Pang et al., 1983).

Our findings support the observations from the literature that oxygen is an important modulator of cell function. Less clear, however, are the mechanisms by which cells sense and respond to the local oxygen environment. In the case of hypoxia-dependent changes in gene expression in which the heterodimeric transcription factor HIF-1α plays a major role, heme proteins have been suggested as the purported oxygen sensor. Though no ubiquitous heme molecule has been identified as an oxygen sensor, observations that transition metals (Co, Ni, and Mn) and iron chelators induce HIF-1α while competitive heme binding by CO or NO reduces HIF-1α activity support this hypothesis (Maxwell and Ratcliffe, 2002). In addition, hydrogen peroxide may act a second messenger downstream of a heme binding event to modulate transcription factor binding (Jungermann and Kietzmann, 2000). Exogenously added H_2O_2 in hepatocyte cultures paralleled the effect of periportal oxygen by enhancing the glucagon-dependent induction of PEPCK while in HeLa cells H_2O_2 resulted in destabilization of HIF-1α (Huang et al., 1996; Kietzmann et al., 1996). The heme-based O_2 sensing model is consistent with the modulation of the PEPCK via a normoxia response element (Bratke et al., 1999), but HIF-1α has not yet been implicated in the oxygen-dependent regulation of CYP2B expression, suggesting a more direct role of heme proteins in CYP gene expression (Kietzmann et al., 1999). Independent of the mechanism, however, the gradient system presented here can provide a continuous range of oxygen tensions in which the functional range of candidate oxygen sensors may be determined.

In summary, we have constructed a bioreactor that allows steady-state oxygen gradients to be imposed upon in vitro culture systems. We have applied this chamber to liver zonation and have shown that physiological oxygen gradients contribute to heterogeneous induction of PEPCK and CYP2B that mimics distributions in vivo. Our results demonstrate the ability of oxygen to modulating gene expression and imply that oxygen plays an important role in the maintenance of liver-specific metabolism in a bioreactor system. In addition, considerations of the effect of oxygen gradients in the design and optimization current bioartificial support systems may serve to improve their function (Allen et al., 2001). Other applications of the gradient system might involve examination of ischemia-reperfusion injury, the mechanisms of ischemic preconditioning being attempted in organ preservation (Peralta et al., 1997), and mechanisms of

zonal toxicity such as that caused by carbon tetrachloride or acetaminophen (de Groot and Littauer, 1989). This approach is generally applicable to systems that can benefit from (i) a continuous range of O_2 concentration; (ii) dynamics; (iii) large cell populations for molecular characterization; and (iv) the role flow and soluble factors on cell function

References

Allen JW, Hassanein T, Bhatia SN. 2001. Advances in bioartificial liver devices. Hepatology 34:447–455.

Bader A, Knop E, Böker K, Frühauf N, Schüttler W, Oldhafer K, Burkhard R, Pichlmayr R, Sewing KF. 1995. A novel bioreactor design for in vitro reconstruction of in vivo liver characteristics. Artif Organs 19: 368–374.

Baron J, Redick JA, Guengerich FP. 1981. An immunohistochemical study on the localization and distributions of phenobarbital- and 3-methylcholanthrene-inducible cytochromes P-450 within the livers of untreated rats. J Biol Chem 256:5931–5937.

Bhatia SN, Balis UJ, Yarmush ML, Toner M. 1999. Effect of cell–cell interactions in preservation of cellular phenotype: cocultivation of hepatocytes and nonparenchymal cells. FASEB J 13:1883–1900.

Bratke J, Kietzmann T, Jungermann K. 1999. Identification of an oxygen-responsive element in the 5′-flanking sequence of the rat cytosolic phosphoenolpyruvate carboxykinase-1 gene, modulating its glucagon-dependent activation. Biochem J 339:563–569.

Custer L, Mullon CJ. 1998. Oxygen delivery to and use by primary porcine hepatocytes in the HepatAssist 2000 system for extracorporeal treatment of patients in end-stage liver failure. Adv Exp Med Biol 454: 261–271.

D'Angio CT, Finkelstein JN. 2000. Oxygen regulation of gene expression: a study in opposites. Mol Genet Metab 71:371–380.

de Groot H, Littauer A. 1989. Hypoxia, reactive oxygen, and cell injury. Free Radical Biol Med 6:541–551.

Foy BD, Rotem A, Toner M, Tompkins RG, Yarmush ML. 1994. A device to measure the oxygen uptake rate of attached cells—importance in bioartificial organ design. Cell Transplantation 3:515–527.

Giffin BF, Drake RL, Morris RE, Cardell RR. 1993. Hepatic lobular patterns of phosphoenolpyruvate carboxykinase, glycogen synthase, and glycogen phosphorylase in fasted and fed rats. J Histochem Cytochem 41:1849–1862.

Giordano FJ, Johnson RS. 2001. Angiogenesis: the role of the microenvironment in flipping the switch. Curr Opin Genet Dev 11:35–40.

Harris AL. 2002. Hypoxia—a key regulatory factor in tumour growth. Nat Rev Cancer 2:38–47.

Hay PD, Veitch AR, Gaylor JD. 2001. Oxygen transfer in a convection-enhanced hollow fiber bioartificial liver. Artif Organs 25:119–130.

Hellkamp J, Christ B, Bastian H, Jungermann K. 1991. Modulation by oxygen of the glucagon-dependent activation of the phosphoenolpyruvate carboxykinase gene in rat hepatocyte cultures. Eur J Biochem 198:635–639.

Herman B, Nieminen AL, Gores GJ, Lemasters JJ. 1988. Irreversible injury in anoxic hepatocytes precipitated by an abrupt increase in plasma membrane permeability. FASEB J 2:146–151.

Huang LE, Arany Z, Livingston DM, Bunn HF. 1996. Activation of hypoxia-inducible transcription factor depends primarily upon redox-sensitive stabilization of its alpha subunit. J Biol Chem 271: 32253–32259.

Jungermann K, Kietzmann T. 2000. Oxygen: modulator of metabolic zonation and disease of the liver. Hepatology 31:255–260.

Jungermann K, Thurman RG. 1992. Hepatocyte heterogeneity in the metabolism of carbohydrates. Enzyme 46:33–58.

Kietzmann T, Freimann S, Bratke J, Jungermann K. 1996. Regulation of the gluconeogenic phosphoenolpyruvate carboxykinase and glycolytic aldolase A gene expression by O_2 in rat hepatocyte cultures. Involvement of hydrogen peroxide as mediator in the response to O_2. FEBS Lett 388:228–232.

Kietzmann T, Hirsch-Ernst KI, Kahl GF, Jungermann K. 1999. Mimicry in primary rat hepatocyte cultures of the in vivo perivenous induction by phenobarbital of cytochrome P-450 2B1 mRNA: role of epidermal growth factor and perivenous oxygen tension. Mol Pharmacol 56: 46–53.

Kietzmann T, Jungermann K. 1997. Modulation by oxygen of zonal gene expression in liver studied in primary rat hepatocyte cultures. Cell Biol Toxicol 13:243–255.

Ledezma GA, Folch A, Bhatia SN, Balis UJ, Yarmush ML, Toner M. 1999. Numerical model of fluid flow and oxygen transport in a radial-flow microchannel containing hepatocytes. J Biomech Eng 121:58–64.

Lindros KO. 1997. Zonation of cytochrome P450 expression, drug metabolism and toxicity in liver. Gen Pharmacol 28:191–196.

Maxwell PH, Ratcliffe PJ. 2002. Oxygen sensors and angiogenesis. Semin Cell Dev Biol 13:29–37.

Murtagh MT, Kwon HC, Shahriari MR, Krihak M, Ackley DE. 1998. Luminescence probing of various sol–gel hosts with a Ru(II) complex and the practical ramifications for oxygen-sensing applications. J Mater Res 13:3326–3331.

Pang KS, Koster H, Halsema IC, Scholtens E, Mulder GJ, Stillwell RN. 1983. Normal and retrograde perfusion to probe the zonal distribution of sulfation and glucuronidation activities of harmol in the perfused rat liver preparation. J Pharmacol Exp Ther 224:647–653.

Peralta C, Hotter G, Closa D, Gelpi E, Bulbena O, Rosello-Catafau J. 1997. Protective effect of preconditioning on the injury associated to hepatic ischemia–reperfusion in the rat: role of nitric oxide and adenosine. Hepatology 25:934–937.

Powers MJ, Domansky K, Kaazempur-Mofrad MR, Kalezi A, Capitano A, Upadhyaya A, Kurzawski P, Wack KE, Stolz DB, Kamm R, Griffith LG. 2002. A microfabricated array bioreactor for perfused 3D liver culture. Biotechnol Bioeng 78:257–269.

Press WH. 1992. Partial differential equations. In: Numerical recipes in FORTRAN: the art of scientific computing. New York: Cambridge University Press. p 838–844.

Sargent BJ, Gough DA. 1991. Design and validation of the transparent oxygen sensor array. IEEE Trans Biomed Eng 38:476–482.

Seglen PO. 1976. Preparation of isolated rat liver cells. Methods Cell Biol 13:29–83.

Semenza GL. 1999. Regulation of mammalian O_2 homeostasis by hypoxia-inducible factor 1. Annu Rev Cell Dev Biol 15:551–578.

Tilles AW, Baskaran H, Roy P, Yarmush ML, Toner M. 2001. Effects of oxygenation and flow on the viability and function of rat hepatocytes co-cultured in a microchannel flat-plate bioreactor. Biotechnol Bioeng 73:379–389.